τ_0 = average residence time = $L/\bar{v}$
φ = quantum yield of initiation step, g.mole/(Einstein)

Subscripts

i = component
r = radial distance
z = axial distance

LITERATURE CITED

1. Benson, S. W., "The foundation of Chemical Kinetics" Butterworth's (1963).
2. ———, *J. Chem. Phys.*, **20**, 1605 (1962).
3. Benson, S. W., *Advan. Photochemistry*, **2**, 1 (1964).
4. Bruce, G. H., D. M. Peaceman, H. H. Rachford, Jr., and J. D. Rice, *Am. Inst. Mining Met. Engrs., Petroleum Trans.* **198**, 79 (1953).
5. Calvert, J. G., and J. N. Pitts, Jr., "Photochemistry," John Wiley, New York (1966).
6. Cassano, A. E., and J. M. Smith, *AIChE J.*, **12**, 1124 (1966).
7. Cleland, F. A., and R. H. Wilhelm, *ibid.*, **2**, 489 (1956).
8. Crank, J., and P. N. Nicholson, *Proc. Cambridge Phil. Soc.*, **43**, 50 (1947).
9. Doede, C. M., and C. A. Walker, *Chem. Eng.* **62**, 159 (1959).
10. Foraboshi, F. P., *Chem. Ind. (Milan)*, **41**, 731 (1959).
11. Gaertner, R. F., and J. A. Kent, *Ind. Eng. Chem.*, **50**, 1223 (1958).
12. Hill, F. B., and R. M. Felder, *AIChE J.*, **11**, 873 (1965); Hill, F. B., and N. Reiss, paper presented at 16th Annual Canadian Chem. Eng. Conference, Windsor, Ontario (Oct. 1966).
13. Huff, J. E., C. A. Walker, *AIChE J.*, **8**, 193 (1962).
14. Lapidus, L., "Digital Computation for Chemical Engineers," McGraw-Hill, New York (1962).
15. Ravinovitch, B. S., and D. W. Setser, *Advan. Photochemistry*, **3**, 1 (1964).
16. Schechter, R. S., and E. H. Wissler, *Appl. Sci. Res., Sect. A:* **9**, 334 (1960).

Manuscript received September 16, 1967; revision received October 12, 1967; paper accepted October 16, 1967.

The Dynamic Behavior of a Packed Liquid Extraction Column

JOSEPH E. DONINGER

International Minerals and Chemical Corporation, Libertyville, Illinois

and WILLIAM F. STEVENS

Northwestern University, Evanston, Illinois

The dynamic behavior of a packed liquid extraction column was investigated by comparing experimental frequency response data obtained from pulse testing with theoretical frequency response data. The theoretical model, which assumed that the column can be represented by a series of perfectly mixed cells, did not adequately describe the frequency response characteristics of the extraction process. However, by the utilization of various magnitude and phase correction factors, a technique was developed to obtain a semiempirical model that could be used to duplicate the actual performance of the liquid extraction column.

In the past few years various attempts have been made to extend the frequency response method of analysis to countercurrent mass transfer operations. Gray and Prados (*9, 10*) have presented a thorough theoretical and experimental investigation of the dynamic behavior of a packed gas absorption column in which carbon dioxide is absorbed from air by water. The frequency response data were obtained by direct sinusoidal forcing of the carbon dioxide input concentration of the gas stream. Several models such as the slug flow, mixing cell, and axial diffusion models were proposed to describe the dynamic behavior of the gas absorption column. Comparison of theoretical and experimental results showed that none of the models completely characterized the gas absorption process. Doninger and Stevens (*3, 4*) proposed that a graphical, semiempirical method be used to describe the frequency response characteristics of a packed gas absorption column.

The first application of arbitrary pulse forcing techniques to obtain frequency response data for chemical engineering processes was made by Lees and Hougen (*13*) in the study of heat exchanger dynamics. Hougen and Walsh (*11*) extended the use of this technique to determine the dynamic behavior of pneumatic control systems, heat exchangers, differential refractometers, and liquid mixing vessels. Watjen and Hubbard (*18, 19*) investigated the dynamics of liquid extraction for a pulsed plate extraction column in which methyl isobutyl ketone was used to extract acetic acid from water. The mass transfer and fluid flow dynamics were excited by injecting a rectangular pulse of acid of short duration into the water phase above the top plate of the column. Samples of the raffinate were taken until the column returned to steady state conditions. The raffinate samples were analyzed by titration and the transient response data were reduced to frequency response data by numerical integration using rectangular area approximation methods. Experiments were also conducted in which only the fluid flow dynamics were excited. The experimental results in the mixer-settler flow region of low column pulse frequency were found to be in good agreement with the linear model theory.

It was the work of Watjen and Hubbard (*18, 19*) which suggested the application of the pulse forcing technique to determine the dynamic behavior of the liquid extraction column. It was felt, however, that an improvement could be made in the type of concentration pulse used to excite the mass transfer dynamics and in the approximation methods used for data reduction. In Watjen's pulse experiments, 2 cc. of pure acetic acid were injected into the system over a period of 1 sec. This caused a high instantaneous concentration of acid in the aqueous phase above the top plate of the column. In the pulse experiments conducted in this study, a rectangular acetic acid pulse with a longer duration but lower concentration was used to minimize the introduction of non-

linearities to the dynamic behavior of the liquid extraction column.

The numerical methods available for reducing the experimental pulse date to frequency response data have been thoroughly investigated by Clements and Schnelle (*2*). Of all the formulas investigated, Filon's quadrature formulas (*8*) proved to be superior for the recovery of frequency response data. It was therefore decided to use Filon's quadrature formulas to evaluate the integrals encountered in analyzing the experimental pulse data (*5*).

THEORETICAL FREQUENCY RESPONSE ANALYSIS

The theoretical model used to describe the liquid extraction process is the mixing cell model. In this model, the liquid extraction column is represented by a series of noninteracting, perfectly mixed cells. The mixing cell model was first used by Kramers and Alberda (*12*) to describe axial mixing in a single phase system. Gray and Prados (*9, 10*) extended the concept to include two phase absorption systems.

An example of a mixing cell is shown in Figure 1. Applying the law of conservation to the solute component for the nth mixing cell for the two phases yields:

$$x_{n-1}L - x_nL - QaH = Hh_L\frac{dx_n}{dt} \tag{1}$$

$$y'_{n+1}G - y'_nG + QaH = Hh_G\frac{dy'_n}{dt} \tag{2}$$

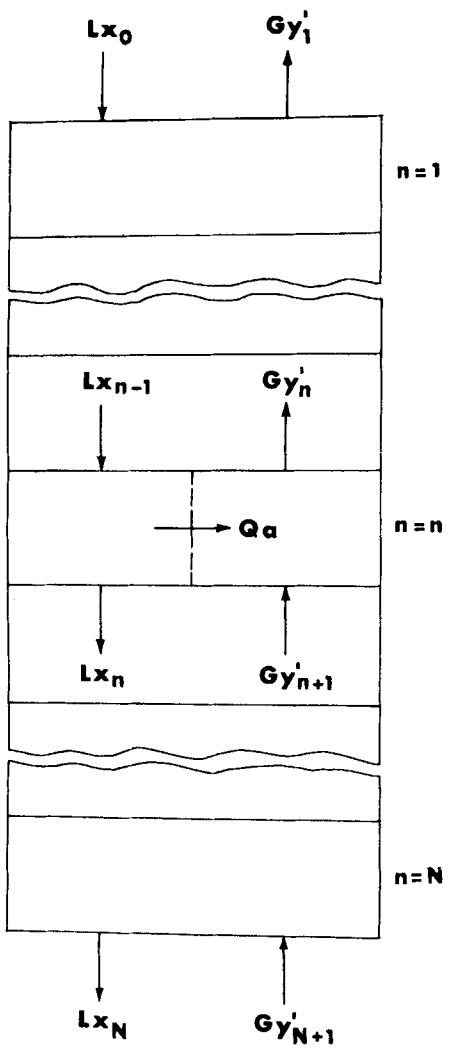

Fig. 1. Mixing cell model of liquid extraction column.

Equations (1) and (2) assume that L, G, h_L and h_G are constant and H is the same for both the water and organic phases.

The variation of interphase mass transfer with concentration is described by the Lewis Model (*6*):

$$Qa = k_La\,(x_n - x_n^*) \tag{3}$$

A plot of the equilibrium data available on the distribution of acetic acid between the water and organic phases (*1, 7, 15* to *17*) yields the following straight line relationship:

$$y' = mx^* - b = 0.766x^* - 0.0056 \tag{4}$$

where

$$0.02 < y' < 0.10$$

After introducing a change in scale of the organic phase composition, $y_n = y_n' + b$, and taking the Laplace transformation of Equations (1) through (4), the following second-order, transformed, difference equation is obtained (*9, 5*).

$$T_L\bar{x}_{n+2} - (T_LT_G - fg + 1)\bar{x}_{n+1} + T_G\bar{x}_n = 0 \tag{5}$$

where

$$T_L = \frac{Hh_Ls}{L} + \frac{Hk_La}{L} + 1 \qquad f = \frac{Hk_La}{mL}$$

$$T_G = \frac{Hh_Gs}{G} + \frac{Hk_La}{mG} + 1 \qquad g = \frac{Hk_La}{G}$$

Since the composition variables are measured as deviations from their steady state values, the boundary conditions for the sinusoidal water phase composition and for the constant organic phase composition are

$$\bar{x}_n = \bar{x}_0 \text{ at } n = 0 \tag{6}$$

$$\bar{y}_{n+1} = 0 \text{ at } n = N$$

Solving Equation (5) with the boundary conditions given in Equation (6) yields the following transfer function for the water phase of the liquid extraction column:

$$G(s) = \frac{\bar{x}_N}{\bar{x}_0} = \frac{T_G{}^N\sqrt{(T_LT_G - fg + 1)^2 - 4T_LT_G}}{T_LT_G(D_2{}^N - D_1{}^N - D_2{}^{N-1} + D_1{}^{N-1}) - fg(D_2{}^N - D_1{}^N)} \tag{7}$$

where

$$D_{1,2} = \frac{(T_LT_G - fg + 1 \pm \sqrt{(T_LT_G - fg + 1)^2 - 4T_LT_G}}{2}$$

The frequency response data are obtained from the transfer function by substitution of $i\omega$ for s, and then, by extracting the magnitude ratio and phase shift from the resulting complex number (*9, 14*). By rewriting Equation (7) in polar form (*5*) we obtain

$$G(i\omega) = \frac{\bar{x}_N(i\omega)}{\bar{x}_0(i\omega)} = \frac{Ae^{\theta_A i}}{Be^{\theta_B i} - Ce^{\theta_C i}} \tag{8}$$

In a previous study, Gray (*9*) obtained the same type of transfer function when he used the mixing cell model to describe the dynamic behavior of a gas absorption column. However, in his analysis it could be assumed that the term $(Ce^{\theta_C i})$ was negligible. In liquid extraction this

simplification cannot be made (5).

After multiplying the denominator by its complex conjugate and using the trigonometric subtraction formulas, Equation (8) becomes

$$G(i\omega) = u + iv = Me^{i\phi} \tag{9}$$

where

$$M = \sqrt{u^2 + v^2}$$

$$\phi = \tan^{-1}\frac{v}{u}$$

$$u = \frac{AB\cos(\theta_A - \theta_B) - AC\cos(\theta_A - \theta_C)}{B^2 + C^2 - 2BC\cos(\theta_B - \theta_C)}$$

$$v = \frac{AB\sin(\theta_A - \theta_B) - AC\sin(\theta_A - \theta_C)}{B^2 + C^2 - 2BC\cos(\theta_B - \theta_C)}$$

The dynamic behavior of the liquid extraction column, as described by the mixing cell model, can now be completely characterized by determining the magnitude ratio, M, and phase shift, ϕ, as a function of the frequency (5).

EXPERIMENTAL FREQUENCY RESPONSE ANALYSIS

In frequency response analysis the two most common ways to determine dynamic behavior of a process are by direct sinusoidal forcing and by arbitrary pulse forcing. From a practical standpoint, obtaining the frequency response characteristics by direct sinusoidal forcing has many disadvantages. The most important disadvantage is that the tests are very time consuming and cause many problems with the normal operation of a process. Furthermore, sinusoidal function generators which operate over a wide range of frequencies are usually very difficult to build.

A more efficient method for obtaining the frequency response data is to analyze the transient response of a process to an arbitrary pulse input. A pulse is a function which differs from its steady state value for only a finite period of time. The main requirement is that the pulse be large enough to excite the dynamics of the process without causing nonlinearities. When applying the pulse forcing technique, the primary advantage is that the complete frequency response of the process can be determined from one pulse test. This is because the pulse function excites all dynamic frequencies of the process simultaneously. Frequency response data obtained through pulse forcing techniques are identical with those obtained by direct sinusoidal forcing techniques when the system is linear (11).

The mass transfer dynamics of the liquid extraction column were excited by injecting acetic acid into the water feed stream in such a manner as to approximate a rectangular pulse of concentration. As will be explained later in this section, the rectangular pulse was chosen because the pulse did not have to correspond to any definite mathematical shape. During the preliminary studies on the size of the rectangular pulse, it was found that the response of the liquid extraction column was sensitive to the concentration of the acid injected into the water feed stream. When pure acetic acid was used, acid was plainly visible in the methyl-isobutyl-ketone phase above the packing. This indicated that the acid did not mix well with the water and that the column was forced into an abnormal mode of operation. To eliminate the problem of introducing nonlinearities, the acetic acid was diluted to a concentration of 28 wt. % before injection into the water feed stream. The actual concentration of acid pulse after mixing with the water feed stream was held constant at 17 wt. % by adding the same amount of acid in each test and altering the input pulse period and water feed flow rate.

Since the liquid extraction column is a stable system, the response of the raffinate concentration to the rectangular input pulse was also a pulse, but with a much larger period and no definite mathematical form. The dynamic mass transfer behavior of the liquid extraction column was determined by reducing the transient response data to frequency response data. The experimental transfer function for the liquid extraction column can be written as

$$G(s) = \frac{\bar{x}_{out}(s)}{\bar{x}_{in}(s)} = \frac{\bar{x}'_{out}(s)e^{-T_d s}}{\bar{x}_{in}(s)} \tag{10}$$

The magnitude and phase of the transform of the input pulse were determined by direct integration of the rectangular function. Thus

$$\bar{x}_{in}(s) = \frac{\bar{x}_{in}(1 - e^{-T_{in}s})}{s} \tag{11}$$

Substitution of $i\omega$ for s and extraction of the magnitude, M_{in}, and phase, θ_{in}, yields the following complex number in polar form:

$$\bar{x}_{in}(i\omega) = \frac{2x_{in}}{\omega}\sin\left(\frac{\omega T_{in}}{2}\right)e^{-\frac{i\omega T_{in}}{2}} = M_{in}e^{i\theta_{in}} \tag{12}$$

The magnitude and phase of the transform of the response function were found by numerically integrating the numerator of Equation (10) after substituting $i\omega$ for s and applying the trigonometric identity for $e^{-i\omega t}$:

$$\bar{x}'_{out}(i\omega) = \int_o^{T_{out}} x_o(t)\cos\omega t\,dt - i\int_o^{T_{out}} x_o(t)\sin\omega t\,dt \tag{13}$$

Since $\bar{x}'_{out}(i\omega)$ is a complex number, Equation (13) can also be written in polar form:

$$\bar{x}'_{out}(i\omega) = M_{out}e^{i\theta_{out}} \tag{14}$$

Substitution of Equations (12) and (14) into Equation (10) yields

$$G(i\omega) = \frac{\bar{x}_{out}(i\omega)}{\bar{x}_{in}(i\omega)} = \frac{M_{out}}{M_{in}}e^{i(\theta_{out} - \theta_{in} - \omega T_d)} = Me^{i\phi} \tag{15}$$

where

$$M = M_{out}/M_{in}$$

$$\phi = \theta_{out} - \theta_{in} - \omega T_d$$

The experimental dynamic behavior of the liquid extraction column can now be characterized by determining the magnitude ratio, M, and phase shift, ϕ, as a function of frequency.

The integrals in Equation (13) could not be evaluated by ordinary numerical methods, such as the trapezoidal rule or Simpson's rule, because the results are not reliable at high frequencies where the sinusoidal functions oscillate rapidly. Clements and Schnelle (2) have recommended that Filon's quadrature formulas (8) be used to evaluate these integrals. Filon's formulas give a parabolic approximation to the response curve that is accurate over all frequencies. Filon's formulas were programmed for use on an IBM 709 computer along with the necessary equations for determining the complete experimental frequency response of the liquid extraction column (5).

The range of useful frequency response information obtained from pulse testing depends on both the type and the duration of the input pulse used to excite the dynamics of the process. If the duration of the pulse is long in com-

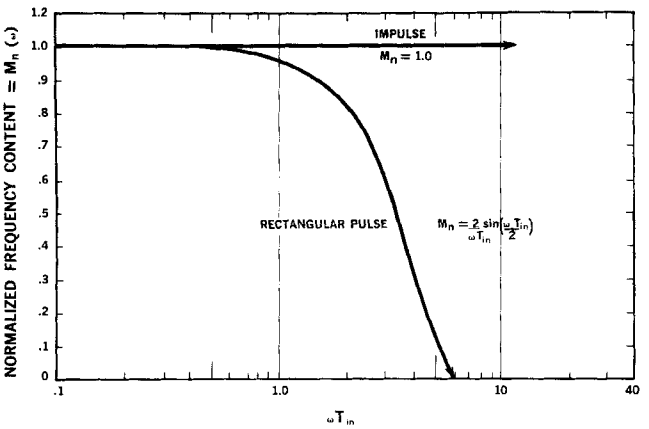

Fig. 2. Frequency content of the rectangular and impulse functions.

parison with the duration of the response, only the lower frequencies of the process are excited. To excite the higher frequencies, it is necessary to decrease the duration of the pulse and increase the pulse height.

The effect of the type of pulse used to obtain the frequency response information is investigated by plotting the normalized frequency content of the pulse, $M_n(\omega)$, as a function of the frequency and the pulse width, ωT_{in} (*2, 11*). The normalized frequency content of the rectangular pulse, from Equation (12), is

$$M_n(\omega) = \frac{M_{in}(\omega)}{M_{in}(o)} = \frac{2}{\omega T_{in}} \sin\left(\frac{\omega T_{in}}{2}\right) \qquad (16)$$

In Figure 2 the normalized frequency content of the rectangular pulse is compared with the normalized frequency content of the impulse function. The importance of the impulse function should not be underestimated because it is the only function which has a normalized frequency content of unity for all frequencies from zero to infinity. The frequency content of all other pulse functions changes with frequency.

The frequency content of different pulses can be compared by locating the frequency at which $M_n(\omega)$ reaches its first zero. The first zero of the rectangular pulse occurs when $\omega T_{in} = 2\pi$. It is important to know where the first zero of $M_n(\omega)$ occurs, for a given pulse, when evaluating the response of a process by numerical methods. Clements and Schnelle (*2*) and Hougen and Walsh (*11*) have shown in previous studies that the integration formulas give reliable frequency response information out to a frequency where $M_n(\omega)$ drops below a value of 0.30. This is a practical limitation which is encountered because of the sensitivity of numerical approximation methods to truncation and round off errors. If it is necessary to increase the useful range of the frequency response information, a pulse with a higher frequency content should be used.

As was mentioned before, the useful frequency range of a pulse can also be extended by decreasing the pulse width. For a given pulse shape and value of $M_n(\omega)$ in Figure 2, ωT_{in} remains constant but T_{in} can be reduced to extend the frequency range. However, an experimental limitation is soon reached because a large pulse height would be needed to obtain a measurable process response.

The type of pulse that is used to excite the dynamics of the process should depend only on the dynamic characteristics inherent in the process. If the dynamic response of the process to high frequencies is important, pulses with a higher frequency content should be used. In certain processes with large time lags, such as the liquid extraction column, only the lower frequencies are important. In this case the rectangular pulse can be used to approximate the impulse function. Referring again to Figure 2, the frequency content of the impulse and the rectangular pulse are almost identical when ωT_{in} is less than 0.40. If the important frequency response characteristics of the process response are at values of ωT_{in} below 0.40, the pulse used to excite the dynamics of the process need not conform to any definite mathematical shape. The pulse is then relatively easy to generate because it is necessary to know only the area under the pulse curve.

It is important to realize that there are now two limiting factors involved in obtaining the useful range of frequency response information from pulse testing. The first is the limiting frequency which occurs when $M_n(\omega)$ of the input pulse drops below a value of 0.30 and is the result of errors inherent in numerical approximation methods. The second is the limiting frequency at which the pulse used to excite the dynamics of the system can no longer be approximated by the rectangular function (*5*). In Figure 2 the second limiting frequency is seen to occur well below the first limiting frequency. However, to extend the range from the first to the second limiting frequency, it is necessary to know the exact mathematical shape of the input pulse. Experimentally, it is difficult to produce a pulse which conforms to a definite mathematical shape.

EXPERIMENTAL APPARATUS AND PROCEDURE

A schematic flow diagram of the liquid extraction equipment is presented in Figure 3. The methyl-isobutyl-ketone and water feed solutions were placed in the constant head tanks at a height of 30 ft. from the top of the liquid extraction column. All lines were ¼ in. O.D. polyethylene tubing with type 316 stainless steel connections. The column was a 64 mm. O.D. (59.2 I.D.-27.2 sq. cm.), standard Pyrex glass tube packed with ¼ in. ceramic Berl saddles to a depth of 91 cm.

The water phase entered the column through the top feed nozzle, 1 in. below the top of the packing. The bottom feed nozzle, which was used to disperse the ketone phase, was imbedded ½ in. into the packing. Because of the difference in densities and the preferential wetting of the packing by the water phase, the ketone rose in droplets through the interstices of the packing. The level of the ketone and water interface during all experimental runs was set at the top of the packing by adjustment of the raffinate and extract microregulating valves.

The unsteady state pulse experiments were conducted after the existence of steady state operation was confirmed. Water and ketone flow rates were maintained at 8.7 and 2.7 wt. % acetic acid, respectively. A 100 cc. hypodermic syringe and a 17 gauge, stainless steel hypodermic needle were used to inject the acetic acid pulse into the water feed stream. The overall flow dynamics were not excited because the water feed flow rate was lowered during the injection of the acid pulse so that the total flow remained constant. As long as the

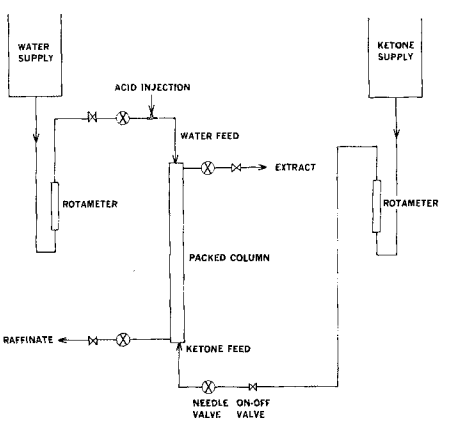

Fig. 3. Schematic flow diagram of experimental apparatus.

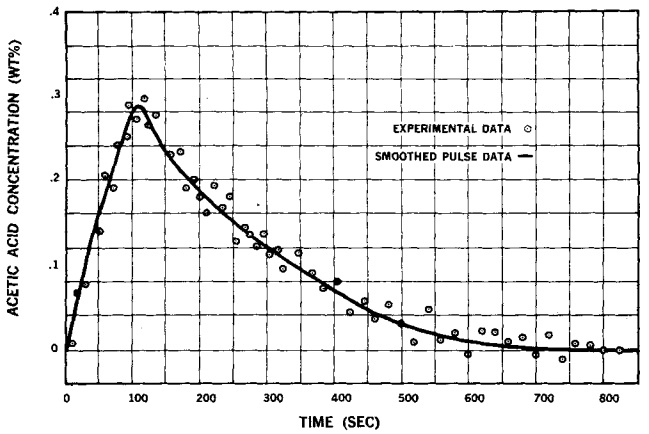

Fig. 4. Experimental pulse data. G = 11.0 g./min.-sq. cm, L = 10.25 g./min.-sq. cm.

level of the liquid-liquid interface did not change, constant total flow conditions could be assumed.

As was mentioned previously, the exact shape of the input pulse curve need not be known. Only the amount of acid added was important. The pulse added to the water feed stream was assumed to be rectangular with a constant pulse height of approximately 0.17 weight fraction of acetic acid. As the water flow rate increased, it was necessary to decrease the duration of the pulse to maintain constant pulse height. For measured water flow rates of 275, 350, and 400 g./min., the pulse duration was 25.5, 20.0, and 17.25 sec., respectively. The ketone flow rates, which were considered to be parameters in these experiments were limited to 295 and 232 g./min. because of the mass transfer characteristics of the liquid extraction column. The actual flow rates used for theoretical calculations and graphs were average values which accounted for the amount of acid transferred from one phase to another. This reduced the maximum error of the flow rate readings to 1.5%.

Samples of the raffinate stream were taken every 10 sec. during the first few minutes of the pulse response. Thereafter, samples were taken every 20 sec. until the column again reached steady state conditions. Approximately fifty to sixty experimental data points were obtained from each run. Continuous response curves were drawn through the experimental data points as shown in Figure 4. The experimental smoothed response data are presented in Table 1* for all flow rate combinations. The experimental frequency response data were then obtained by numerical integration of the transformed response curve [Equation (13)].

The maximum deviation of the response curve from the steady state, raffinate acetic acid concentration decreased with increasing ketone flow rate and/or decreasing water flow rate. For example, at a ketone flow rate of 11.0 g./min. sq. cm. and water flow rate of 10.24 g./min. sq. cm., the maximum deviation from the steady state acid concentration was 0.3 wt. % as compared with a deviation of 1.0 wt. % at a ketone flow rate of 8.65 g./min. sq. cm. and water flow rate of 14.86 g./min. sq. cm. At input pulse magnitudes smaller than 17 wt. % and particularly at the combination of high ketone flow rate with low water flow rate, the experimental data points representing the response of the raffinate stream were too scattered to be separated from normal experimental and analytical deviations. Therefore, to obtain accurate and measurable response curves for all combinations of water and ketone flow rates investigated, the height of the input pulse had to be maintained at 17 wt. %. Although this concentration represented a twofold increase in the steady state acid concentration, it was felt that the introduction of nonlinearities due to changes in physical properties of the system such as solubilities, interfacial tension, etc., would be minimized.

The presence of steady state flow conditions during the pulse testing could be checked by the reading of the rotameters and the level of the liquid-liquid interface. After each run was completed, the water and ketone holdups were determined and the concentrations of the feed and exit streams were checked for verification of steady state conditions. The same procedure was followed by each combination (six in all) of flow rates until reproducible data were obtained. This usually required three experimental runs. From each combination of flow rates, only the results with the least scattering of experimental data points were used.

The temperature of the water and ketone feed solutions varied from 24 to 28°C. as extreme limits. Before each experiment the water and ketone feed solutions were mutually saturated with one another by passing them through the extraction column at maximum flow rates. The concentration of acetic acid in all samples was determined by titration with .1N sodium hydroxide solution to a phenolphthalein end point. The samples were approximately 10 ml. in volume and all ketone samples were mixed with 20 ml. of ethanol to insure complete miscibility with the organic phase. The sodium hydroxide solution was standardized by triplicate titrations, using weighed amounts of dried potassium acid phthalate dissolved in boiled distilled water.

PRESENTATION OF RESULTS

Experimental Steady State Data

The steady state mass transfer coefficient and holdups of the water and ketone phases are shown in Figures 5 through 7 as a function of the water flow rate. In each figure the steady state data are presented with the ketone flow rates as parameters. The equilibrium distribution of acetic acid between the water and methyl isobutyl ketone phases, which holds only over the concentration range of interest, is given by Equation (4) with a change in scale of the organic phase composition, thus

$$y_n = y_n' + 0.0056 = 0.766\, x_n^* \qquad (17)$$

where

$$0.02 < y' < 0.10$$

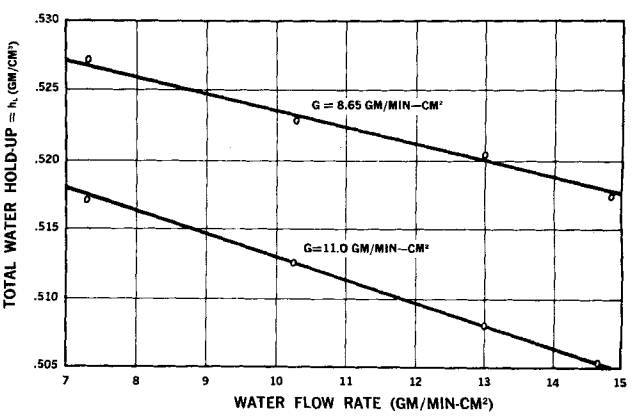

Fig. 5. Effect of water flow rate on the total water holdup.

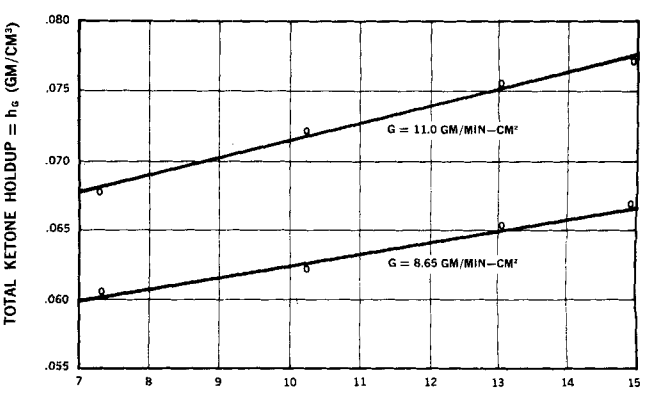

Fig. 6. Effect of water flow rate on the total ketone holdup.

* Table I is deposited as Document 9964 with the American Documentation Institute, Library of Congress, Washington, D. C.

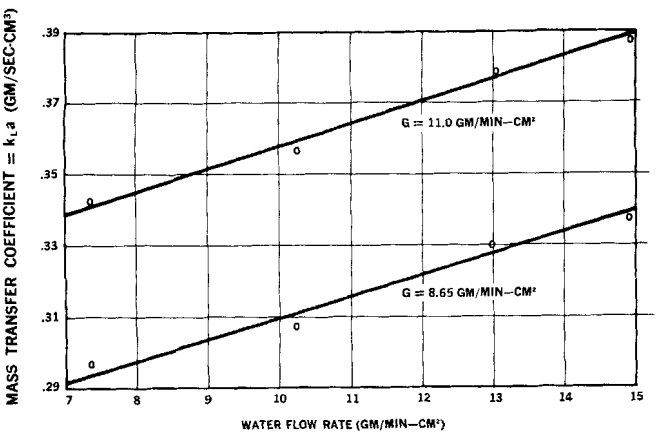

Fig. 7. Effect of water flow rate on the mass transfer coefficient.

Experimental Frequency Response Data

The magnitude ratio for the experimental transfer function is defined as the ratio of the magnitudes of the transforms of the output and input functions and is given by

$$M_e(\omega) = \frac{M_{\text{out}}(\omega)}{M_{\text{in}}(\omega)} \tag{18}$$

It is important to note that the value of the magnitude ratio at zero frequency determines the steady state fraction of acid that remains in the water stream after passing through the column. For easier comparison, the magnitude ratios are presented in normalized form:

$$M_E(\omega) = \frac{M_e(\omega)}{M_E(o)} = \frac{M_{\text{out}}(\omega)/M_{\text{out}}(o)}{M_{\text{in}}(\omega)/M_{\text{in}}(o)} \tag{19}$$

The phase shift for the experimental transfer function is given by

$$\phi_E = \theta_{\text{out}} - \theta_{\text{in}} - \omega T_d \tag{20}$$

The value for the dead time, T_d, was determined in each pulse test by measuring the time lag between the upset of acetic acid concentration in the water feed stream and the response of the acetic acid concentration of the raffinate stream.

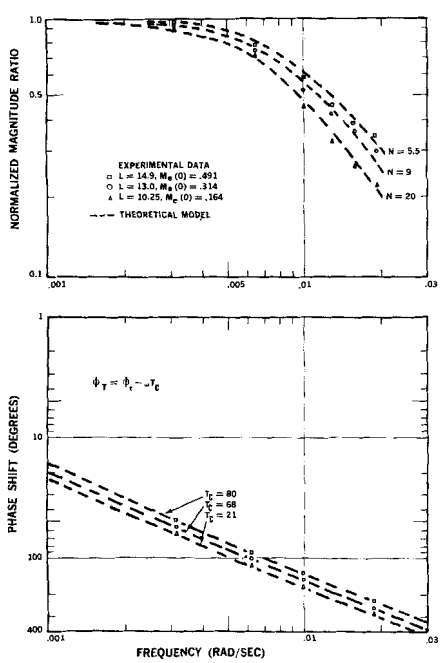

Fig. 8. Comparison of experimental and theoretical frequency response data, G = 11.0 g./min.-sq. cm.

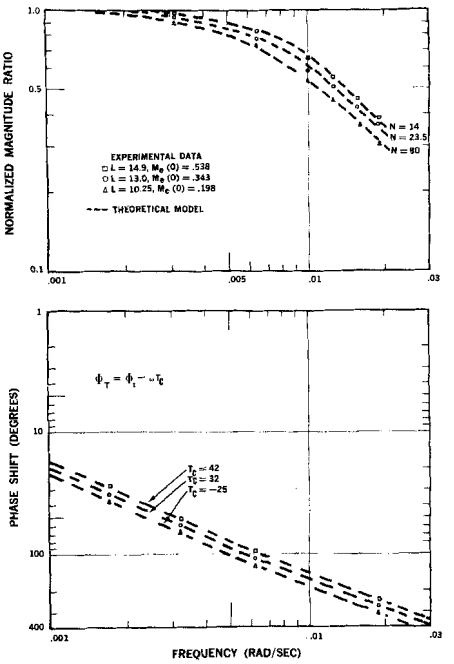

Fig. 9. Comparison of experimental and theoretical frequency response data, G = 8.65 g./min.-sq.cm.

The normalized magnitude ratios and phase shifts are plotted in Figures 8 and 9 as a function of frequency for each combination of flow rates studies. Only the results within the range of experimental reliability of frequency response data are reported.

Theoretical Frequency Response Data

The theoretical frequency response of the liquid extraction column was obtained by substitution of the experimental steady state data into the theoretical frequency response equation, Equation (9). The normalized magnitude ratio of the theoretical transfer function is given by:

$$M_T = \frac{M_t(\omega)}{M_t(o)} \tag{21}$$

The value of the so called "un-normalized" magnitude at zero frequency, $M_t(o)$, determines the theoretical steady state fraction of acid that remains in the water stream after passing through the column. In Figure 10, the normalized magnitude ratio for a particular combination of flow rates is plotted with the number of mixing cells as a parameter. As shown, the number of mixing cells, N, can be varied until good agreement with the experimental magnitude ratios is obtained. Also plotted in Figure 10, is the phase shift for the theoretical transfer function with a phase correction factor as the parameter.

$$\phi_T = \phi_t - \omega T_C \tag{22}$$

where

ϕ_T = corrected theoretical phase shift
ϕ_t = theoretical phase shift, Equation (9)
T_C = phase correction factor

By varying the value of the phase correction factor, agreement can also be obtained with the experimental shift. The technique in Figure 10 was utilized to obtain the theoretical frequency response data for the liquid extraction column. The theoretical results are presented in Figure 8 and 9 for comparison with experimental results.

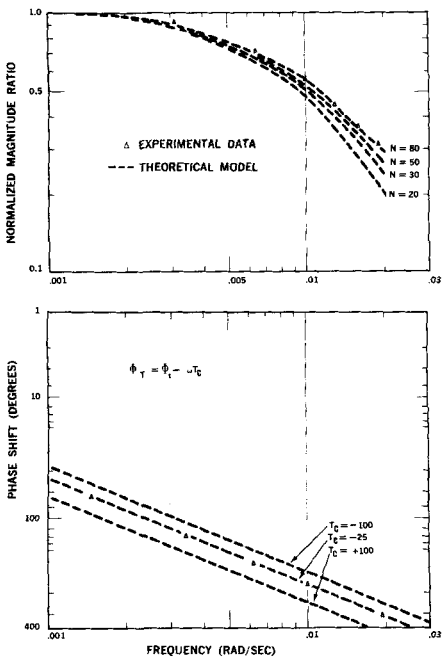

Fig. 10. Technique used to obtain the theoretical frequency response data.

DISCUSSION OF RESULTS

The number of mixing cells, N, for which good agreement was obtained with experimental results is plotted in Figure 11 as a function of the water flow rate with the ketone flow rate as a parameter. These curves were obtained by comparing the experimental and theoretical normalized magnitude ratios, which are given in Figures 8 and 9. The number of mixing cells is shown to decrease with increasing water and ketone flow rates. This type of variation is due to the assumption that the liquid extraction column can be described by a series of perfectly mixed cells. In the liquid extraction column, an increase in the water and ketone flow rates results in an increase in the mixing within the interstices of the packing. The theoretical model accounts for this increased mixing by utilizing fewer mixing cells.

Although the normalized form of the theoretical and experimental magnitude ratios were in good agreement, the un-normalized magnitude ratios did not agree at zero frequency. As was mentioned previously, the un-normalized magnitude ratio determines the steady state fraction of acid that remains in the water phase after passing through the column. The ratio of the un-normalized magnitude ratios at zero frequency is given by

$$C = \frac{M_e(o)}{M_t(o)} = \frac{M_{\text{out}}(o)/M_{\text{in}}(o)}{M_t(o)} \qquad (23)$$

and is called the magnitude correction factor. The value of the magnitude correction factor determines the accuracy of the theoretical model in describing the steady state behavior of the liquid extraction column. If C is greater than 1, the amount of acid extracted from the water stream is less than that predicted by the theoretical model. If C is less than 1, the reverse is true. The magnitude correction factor is plotted in Figure 12 as a function of the water flow rate. Analysis of Figure 12 shows that the deviation between the experimental and theoretical steady state results increases with increasing water flow rate. This can be explained by analyzing the effect of the water flow rate on the type of mixing within the column. As the water flow rate increases, the contact time between the two phases decreases. Since this also decreases the chance for more perfect mixing, the deviation between the experimental results and theoretical model should increase. It is also shown in Figure 12 that the magnitude correction factor decreases when the ketone flow rate is increased. This is explained by the effect of ketone flow on the mixing in the interstices of the column packing. An increase in the ketone flow rate results in an increase in the resistance to the flow of the water phase. This increased flow resistance, in turn, results in better mixing and therefore better mass transfer between the phases.

The value of the phase correction factor required to correct the theoretical phase shift is given by

$$\omega T_C = \phi_t - \phi_E \qquad (24)$$

and is plotted in Figure 13 as a function of the water flow rate. When the phase correction factor is negative the theoretical phase shift lags behind the experimental phase shift. As shown the deviation between the experimental and theoretical phase shifts is smaller at the lower ketone flow rate and increases with increasing water flow rate. The results also show that under most combinations of flow rates investigated, the theoretical phase shift leads the experimental phase shift. The deviation between ex-

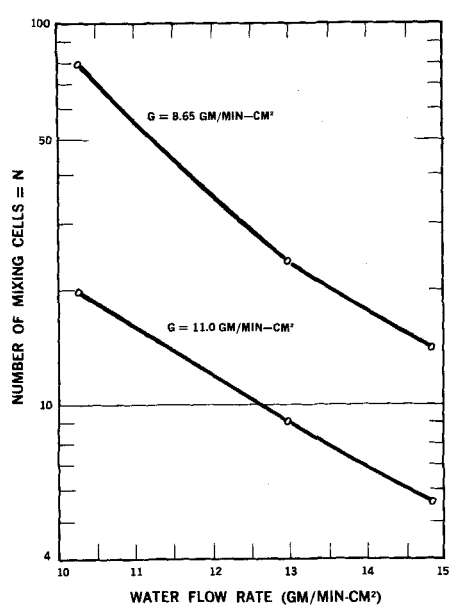

Fig. 11. Variation of the number of mixing cells with the water flow rate.

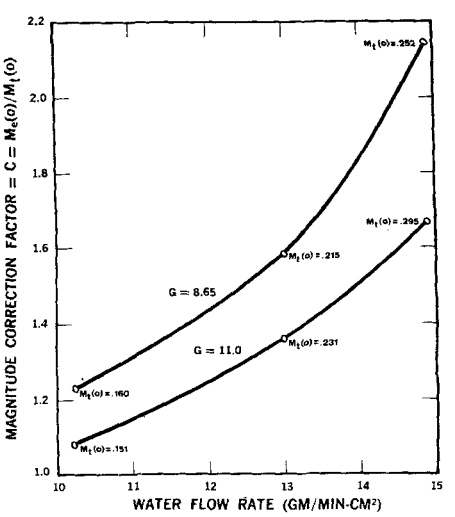

Fig. 12. Variation of the magnitude correction factor with the water flow rate.

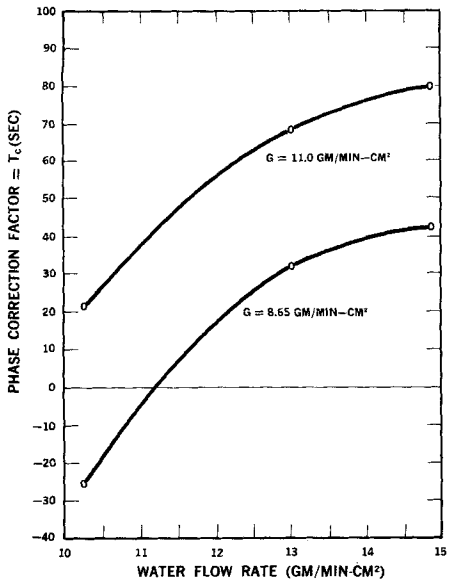

Fig. 13. Variation of the phase correction factor with the water flow rate.

perimental and theoretical results can be explained by the failure of the theoretical model to account for resistance of the droplets of ketone rising through the interstices of the packing on the flow of water. Therefore, when the ketone flow rate is increased, the resistance on the water flow is also increased. Since the phase shift is primarily a measure of the transit time of the acetic acid through the column, the increased resistance would result in an increase in the deviation between experimental and theoretical results.

CONCLUSIONS

Analysis of the theoretical and experimental frequency response data shows that the mixing cell model does not adequately describe the dynamic behavior of the liquid extraction column. If the model was correct, the number of theoretical mixing cells required to approximate the experimental frequency response would remain constant when the flow rates are changed. Also, there would be no need to utilize the magnitude and phase correction factors to correct for the deviation between theoretical and experimental results. It appears possible that a more accurate representation of the mass transfer characteristics of the liquid extraction column would be obtained if mixing cell efficiencies of less than 100% are used. However, the results of this investigation indicate that the mixing cell efficiencies would change when water and ketone flow rates are changed.

The usefulness of the model is not lost because the technique used to compare the theoretical with the experimental results can be used to obtain a semiempirical model for the liquid extraction column. Only two steps have to be followed to obtain the experimental frequency response of the liquid extraction column from the model. The first step is to insert the steady state data and the number of mixing cells from Figure 11 into Equation (9) to obtain the theoretical frequency response. The magnitude and phase correction factors from Figures 12 and 13 can then be used to correct for the deviation between the theoretical model and the experimental results. Although the empirical correlation techniques are valid only for the liquid extraction column employed in this investigation, it should be possible to use the same approach when studying the dynamic behavior of larger columns. Only one pulse test has to be run at each set of flow rates to obtain the experimental frequency response of the column. The phase and magnitude correction factors can then be determined so that the theoretical model can be used to duplicate the dynamic behavior of the column. In many instances, the ability to mathematically describe the actual performance of the liquid extraction column in a chemical process is the most important step of a process control evaluation.

NOTATION

a = mass transfer area, sq. cm./cc. packing
A,θ_A = magnitude and phase of $T_G{}^N\sqrt{(T_LT_G - fg + 1)^2 - 4T_LT_G}$
B,θ_B = magnitude and phase of $T_LT_G\,(D_2{}^N - D_1{}^N - D_2{}^{N-1} + D_1{}^{N-1})$
C,θ_C = magnitude and phase of $fg\,(D_2{}^N - D_1{}^N)$
C = magnitude correction factor, Equation (23)
b = y' intercept of straight equilibrium line
$D_{1,2}$ = $\dfrac{(T_LT_G - fg + 1) \pm \sqrt{(T_LT_G - fg + 1)^2 - 4T_LT_G}}{2}$
f = Hk_La/Lm
g = Hk_La/G
G = organic phase flow rate, g./min.-sq. cm.
$G(s)$ = transfer function
H = packing height equivalent to a mixing cell, cm.
h_G = total organic phase holdup, g./cc. packing
h_L = total water phase holdup, g./cc. packing
k_La = mass transfer coefficient, referred to water phase, g./min.-cc.
L = water phase flow rate, g./min.-sq. cm.
m = distribution coefficient
M_e,M_t = magnitude ratio of the experimental and theoretical transfer functions for the liquid extraction column
M_E,M_T = normalized magnitude ratios of the experimental and theoretical transfer functions
M_{in} = magnitude of experimental input function
M_{out} = magnitude of experimental output function
n = number of the nth mixing cell
N = total number of mixing cells
Q = mass transfer rate, g./min.-sq. cm. transfer area
s = Laplace transform variable
t = time variable, min.
T_d = dead time, Equation (20)
T_{in} = period of input pulse, sec.
T_{out} = period of output pulse, sec.
T_C = phase correction factor, Equation (24)
T_G = $\dfrac{Hh_Gs}{G} + \dfrac{Hk_La}{mG} + 1$
T_L = $\dfrac{Hh_Ls}{L} + \dfrac{Hk_La}{L} + 1$
ω = frequency, rad./sec.
x = mass fraction of acetic acid in water phase, g. acid/g. solution
x^* = mass fraction of acetic acid in equilibrium with the organic phase at the liquid-liquid interface
$\bar{x}, \bar{y}$ = Laplace transform of concentration variables
y' = mass fraction of acetic acid in organic phase, g. acid/g. solution
y = $y' + b$ = mass fraction of acetic acid in organic phase after a change in the concentration scale
z = length dimension, cm.
Z = total packing height, cm.
ϕ_E,ϕ_t = phase shifts of the experimental and theoretical transfer functions
ϕ_T = corrected theoretical phase shift, Equation (22)

LITERATURE CITED

1. Bak, E., and C. J. Geankoplis, *Chem. Eng. Data Ser.*, 3, 256 (1958).
2. Clements, Jr., W. C., and K. B. Schnelle, Jr., *I.E.C. Proc. Des. and Devel.*, 2, 94 (1963).
3. Doninger, J. E., MS thesis, Northwestern Univer., (Aug. 1962).
4. ———, and W. F. Stevens, *Can. J. Chem. Eng.*, 42, 85 (1964).
5. Doninger, J. E., Ph.D. thesis, Northwestern Univer., Evanston, Illinois (June 1965).
6. Edwards, G. A., and D. M. Himmelblau, *Ind. Eng. Chem.*, 53, 229 (1961).
7. Fanning, R. J., and C. M. Sliepcevich, *AIChE J.*, 5, 240 (1959).
8. Filon, L. N. G., *Proc. Roy. Soc. (Edinburgh)*, 49, 38 (1928).
9. Gray, R. I., Ph.D. dissertation, Univ. Tennessee, Knoxville (1961).
10. ———, and J. W. Prados, *AIChE J.*, 9, 211 (1963).
11. Hougen, J. O., and R. A. Walsh, *Chem. Eng. Progr.*, 57, 69 (1961).
12. Kramers, H. and G. Alberda, *Chem. Eng. Sci.*, 2, 173 (1953).
13. Lees, S., and J. O. Hougen, *Ind. Eng. Chem.*, 42, 1048 (1950).
14. Oldenbourg, R. C., and H. Sartorius, "The Dynamics of Automatic Controls," p. 22, Am. Soc. Mech. Eng., New York (1948).
15. Oldshue, J. Y., and J. H. Rushton, *Chem. Eng. Prog.*, 48, 297 (1952).
16. Scheibel, E. G., and A. E. Karr, *Ind. Eng. Chem.*, 42, 1048 (1950).
17. Sobotnik, R. H., and D. M. Himmelblau, *AIChE J.*, 6, 619 (1960).
18. Watjen, J. W., D.Sc. dissertation, Univ. Virginia, Charlottesville (1962).
19. ———, and R. M. Hubbard, *AIChE J.*, 9, 614 (1963).

Manuscript received June 13, 1966; revision received October 12, 1967; paper accepted October 16, 1967.

A Kinetic Theory of Catalysis and Mass Transfer in a Cylinder

L. H. SHENDALMAN

Yale University, New Haven, Connecticut

The diffusion and mass transfer of a trace component in a background gas in a cylinder, is treated according to a relaxation transport equation. The system is assumed isothermal and at rest. An expression for an effective axial diffusivity is found which goes to the appropriate high and low density limits. Numerically, this diffusivity is similar to one half of the harmonic mean of the high density diffusivities, which is often used as an empirical extrapolating formula.

The radial mass transfer problem results in an integral equation which is solved numerically for all Knudsen numbers.

The case of catalytic reaction on the walls is considered in detail. Rarefaction effects become important under conditions of fast reaction. The problem of sublimation or evaporation from a cylinder wall can be treated by the same equations.

The effect of rarefaction (low density) on the utilization of an heterogeneous catalyst is of much interest in the field of chemical reaction engineering. In general, the techniques of Wheeler (7) as described in his pioneering paper do not seem to have been improved upon. An ad hoc approach is used in which a continuum formulation of the diffusion and reaction processes is made. To account for rarefaction, an empirical diffusivity is used which approaches the appropriate limit according to the value of the radial Knudsen number, N_{Kn} which is the ratio of the mean free path to some significant dimension.

The question of the appropriate diffusivity has been studied in some detail (5), and account has been taken of the complex geometric nature of the pore structure of a catalyst; but in most cases the diffusion has been considered separately from the reaction problem.

In recent years tremendous advances have been made in the kinetic theory of rarefied gases. However, only recently has the class of problems called "interior problems" been attacked successfully. The problem of the catalytic conversion of a trace dilute component gas in a cylinder is considered here from the viewpoint of the kinetic theory of gases. The geometry of the cylinder is used although the theory is readily applicable to any constant area, duct geometry.

It has been found that a class of mass transfer problems can be treated in this manner, and sublimation or evaporation is considered.

BACKGROUND

Hamel (4) has considered one dimensional mass transfer problems in perhaps the first rigorous treatment of Knudsen effects in a finite system. He included evaporation and catalysis as examples. Brock (2) has considered the Knudsen layer above a catalytic surface. This is the region roughly one mean path thick above a catalytic surface where the continuum theory has to break down. In